NONLINEAR AND LINEAR PRESSURE DETERMINATION IN A TWO-LAYER STRUCTURE: SOLID CRYSTAL - WATER AT GHZ FREQUENCIES

FILIPCZYŃSKI LESZEK, WÓJCIK JANUSZ, KUJAWSKA TAMARA

Institute of Fundamental Technological Research, Polish Academy of Sciences
Świętokrzyska 21, 00-049 Warsaw, Poland
lfilipcz@ippt.gov.pl

Determination of acoustic pressures at the frequency of 1 GHz by means of PVDF hydrophones is not possible due to their limited frequency response. Moreover, the size of their active electrodes is by about 3 orders of magnitude greater than the resolution in the acoustic microscopes at such a high frequency. Therefore the authors solved this problem at first in a microscope with the working frequency of 34 MHz using both the numerical and experimental methods. A numerical procedure of nonlinear propagation and transducer power measurements were applied giving in effect the same quantitative results. Therefore the identical numerical procedure was used for the 1 GHz microscope working in the reflection mode. Many pressure field quantities of the microscope were shown, e.g. the pressure values, distributions of the first, second, third and forth pressure harmonics in and outside of the focus, pulse distortions and their spectra, the resolutions achieved etc. The obtained information on nonlinear propagation effects in microscopy was previously lacking.

INTRODUCTION

Acoustical imaging of biological structures at the microscope resolution provides foundations of many new biological and medical applications [1]. For these purposes acoustic microscopes operating with the GHz frequencies may be used [9]. Majority of the examined structures such as living cells and soft tissues show acoustical properties similar to those of water. Therefore at the frequency of 1 GHz the wave length is equal to $\lambda = 1.5$ μm. In such a case the determination of the acoustic pressure by means of PVDF hydrophones is not possible since the highest frequency response of those devices is limited to 20 MHz. In the newest, very expensive hydrophones, the upper sensitivity limit is increased to 50 MHz only.

However, the basic limitation of the PVDF hydrophone consists in the size of the active electrode. Its smallest diameter is equal to 0.4 mm, while at the frequency of 1 GHz, the resolution of the order of magnitude of 1 μm is necessary. Concluding one can say that there

is no possibility of acoustic pressure determination by means of the conventional PVDF hydrophone measurement at GHz frequencies.

To solve the problem we decided to find the acoustic pressure values by means of a numerical procedure at the frequency of 1 GHz, solving at first the same problem for a lower frequency of 34 MHz by means of the same numerical algorithm. At this frequency it was also possible to determine the real acoustic pressure by means of an original method based on transducer power measurements [15]. As a result we have obtained the agreement between the computed and experimental pressure values with the accuracy of 2 dB. The calibration uncertainty claimed by producers of PVDF hydrophones at the highest frequency equals ± 2 dB [8].

The obtained agreement between the computed and measured acoustic pressures at the frequency of 34 MHz confirmed the correctness of the applied experimental method and the numerical algorithm. Therefore the same numerical algorithm was applied to the frequency of 1 GHz, assuring in this way that the obtained results were most probable.

For the examination of molecular structures it is necessary to obtain a possibly high resolution. In such a case, at a given frequency, the ultrasonic beam should be strongly focused by the lens incorporated into the solid crystal in the form of a spherical cavity filled with a water-like medium. Therefore, the aperture of this cavity should be high and, in our case, the aperture half-angle was chosen to be $\alpha_m = 50^0$. The ultrasonic beams were generated by transducers in a special lossless crystal glass BK7 used in the 34 MHz microscope and in a sapphire crystal used in the 1 GHz microscope, respectively. Their ends were shaped in the form of a concave spherical lens. Fig. 1 shows the principle of the acoustic microscope satisfying the conditions of very high resolution. The basic parameters of the two microscopes are shown in Table 1.

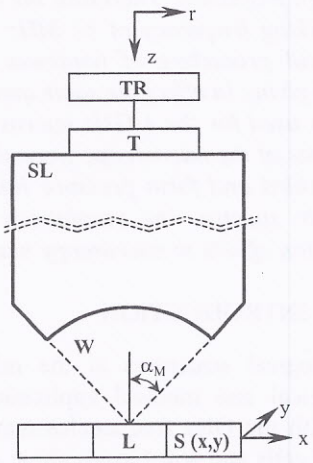

Fig. 1. Principle of the acoustic microscope. TR - transmitting-receiving system, T - transducer, W - water, SL - spherical lens, α_m - aperture half-angle, L - examined object (living tissue), S - scanning system.

1. EXPERIMENTAL DETERMINATION OF ACOUSTIC PRESSURES AT THE FREQUENCY OF 34 MHz

The power supplied at the frequency of 34 MHz to the transducer and the resulting pressure were determined from the measured electrical admittance being equal to $A = (20 + j\ 0.14)$ mS. The radiating circular $LiNBO_3$ transducer, 4.4 mm in diameter, was loaded by glass on one side only. The admittance was determined by means of the admittance bridge, where the spherical lens at the end of the glass medium eliminated standing waves [15]. In this way it was possible to carry out measurements on the used pulses. Table 1 shows the main parameters for assessment of the acoustic pressure on the transducer surface and at the lens input. Since the spherical lens cavity was situated close to the transition zone of the near and far field, the acoustic axial pressure was at the lens input twice higher than assumed at the transducer surface. This was also confirmed by computing the pressure distribution in the beam, as shown in Fig. 2.

Table 1. BASIC PARAMETERS OF THE 34 MHz and 1 GHz MICROSCOPES

1	Carrier frequency of the microscope	MHz	34	1000
2	Absorption in water at 25 °C	Np/mm	0.027	23
3	Wavelength in water	μm	44	1.5
4	Longitudinal and transverse wave speeds in glass	km/s	5.9; 3.6	
5	Longitudinal and transverse wave speeds in sapphire	km/s		11.1; 6.0
6	Acoustic impedance of glass and sapphire	MRayl	13.7	44.4
7	Wavelength in glass and sapphire	μm	173	11.1
8	Discontinuity distance in glass* and sapphire*	mm	107	0.84
9	Transducer – lens front surface distance	mm	30	0.1
10	Discontinuity distance in water	mm	4.3**	0.012***
11	Spherical lens diameter	mm	5.1	0.08
12	Generated power values	W	2.25	0.32
13	Transducers areas (for ∅ = 4.4 mm; ∅ = 34 μm)	m^2	$15.2\ 10^{-6}$	$3.63\ 10^{-9}$
14	Intensity at the transducer	MW/m^2	0.148	88.2
15	Pressure at the transducer	MPa	2.01	88.5
16	Axis pressure at lens input	MPa	4.02	177
17	Lens output axial pressure in water	MPa	0.79	12

* For the average pressure of 3 MPa in glass and 133 MPa in sapphire
** Calculated for the pressure of 1 MPa
*** Calculated for the pressure of 12 MPa corresponding to the transducer power of 0.32 W

It can be verified that due to very high wave velocity, the discontinuity distance [10] for the plane wave in glass and in sapphire was many times greater than the distance between the transducer and the lens surface, equal to the near field limit.

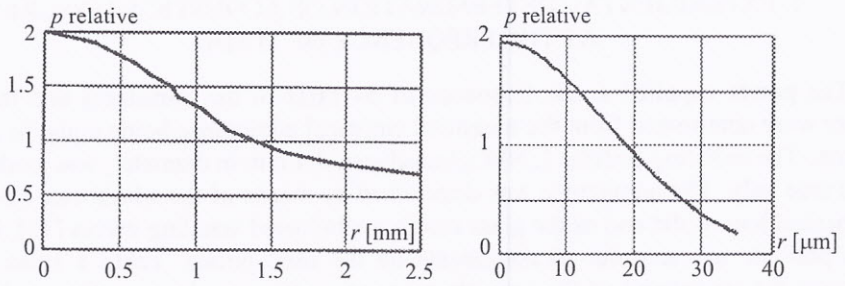

Fig. 2. Radial distribution of the glass (left) and sapphire (right) output pressures computed at the lens surface. The boundary acoustic pressure amplitude (for $z, r = 0$) was assumed to be 1.

For calculations of the discontinuity distance we determined the nonlinear parameter [5] [6]. For sapphire we calculated B/A = 12 while for glass BK7 no information was available, and the same value was assumed. The obtained values of the discontinuity distance (Table 1, line 8)enabled us to apply the linear theory for both crystal media. Moreover, absorption in glass and in sapphire could be practically ignored [2].

However, the low wave velocity and strongly focused field in water, causing very high pressure amplitudes, make it necessary to consider there nonlinear propagation conditions. Also the lens with half-angle apertures exceeding 16^0 can not be described by the simplified theories based on paraxial approximation [11]. In our case the half-angle was equal to 50^0. The discontinuity distance in the water spherical cavity can not be determined by means of formulae used for plane waves as in the case of sapphire and glass. Therefore we used them only as a rough approximation, showing that in water the propagation distance is even greater than the discontinuity one. Therefore, in water the numerical method had to be used to solve this nonlinear problem. In addition, the very high absorption in water at gigahertz frequencies complicated this question.

In the reflection mode, used in both microscopes, the acoustic pulses radiated by the transducers located on the plane surface of the glass and sapphire boundaries, were composed of 4 periods. Their waveform, used in calculations, is shown in Fig. 3.

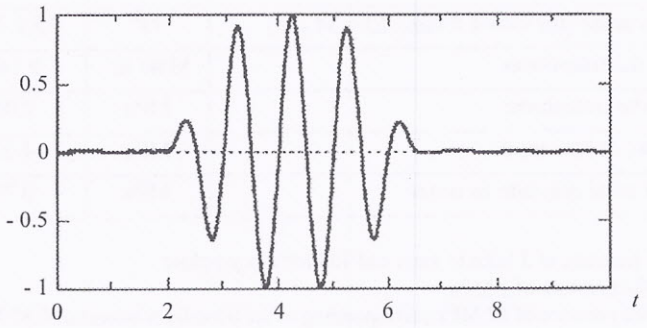

Fig. 3. The waveform of acoustic pulses with the carrier frequencies of 34 MHz and 1 GHz used in computations.

Knowing the supplied power and the transducer diameters, the average intensity could be determined and hence also the corresponding average pressures at the transducer surface. Linear numerical computations of the radiated pulse beam in the glass have shown that the axial pressure at its end, at a distance of 30 mm, was twice as great as that at the transducer surface (Fig. 2). Attenuation in glass was negligibly small. In glass (and in sapphire) linear numerical methods were used, based on typical formulae valid for solid media [7], to describe the boundary pressure distribution on the spherical lens surface. Finally, after penetration of the glass-water boundary, the lens output axial pressure at the boundary in water reached the pressure value of P_w = 0.79 MPa (see Table 1, line 17) according to the simple plane wave formula $P_w = P_g \cdot 2 \cdot \rho_w c_w / (\rho_w c_w + \rho_g c_g)$, where P_g denotes the axial pressure value at the glass boundary, indices g and w concern glass and water, respectively.

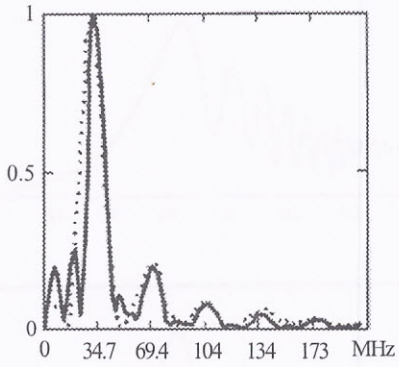

Fig. 4. The computed (solid line) and experimental (dotted line) focal spectra showing an agreement up to the 5-th harmonic.

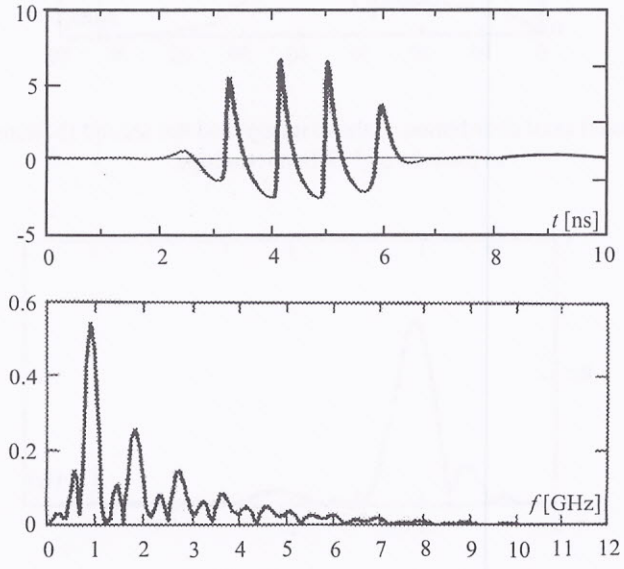

Fig. 5. The 1 GHz pressure pulse distorted due to nonlinear propagation (top) and its amplitude spectrum (bottom), computed in the focus for the high transducer power of 0.32 W.

2. COMPUTATIONS OF ACOUSTIC PRESSURES AT THE FREQUENCY OF 34 MHz

Computations were performed for various pulse pressures causing nonlinear propagation in the water region (Fig. 1). The applied procedure was described in previous papers [12,13] and verified experimentally [3]. After many attempts, finally a pressure amplitude of $P_1 = 1$ MPa at the axis of the output of the spherical lens was found to match the numerically computed focal amplitude spectrum with the experimental one, as shown in Fig. 4 [14]. The numerical results had to be averaged over the surface of the probe used in spectrum measurements. Comparing the computed pressure with the experimental one equal to $P_W = 0.79$ MPa, a small difference of the pressure amplitudes equal to 2 dB was found.

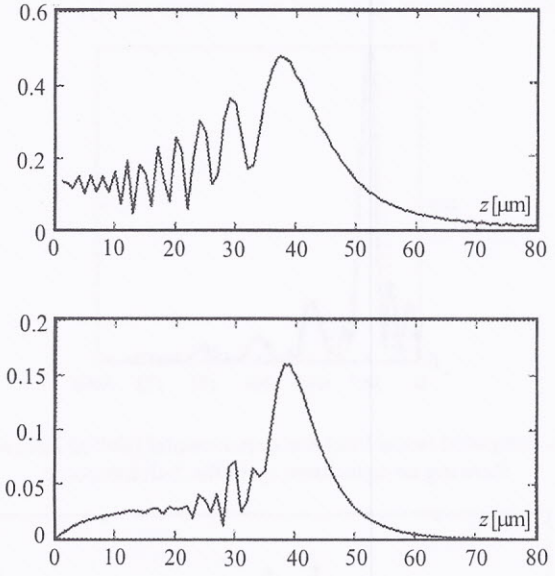

Fig. 6. The computed axial distribution of the first (top) and the second (bottom) harmonics in the case of 1 GHz microscope.

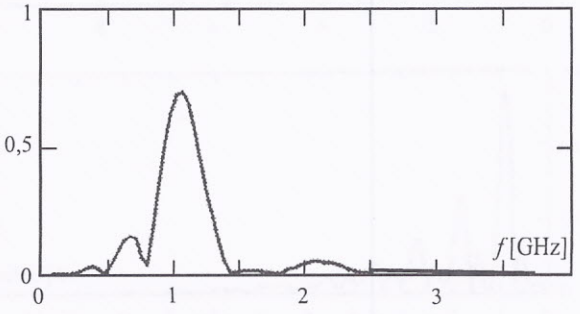

Fig.7. The amplitude spectrum of the 1 GHz pressure pulse computed in the focus for the transducer power 160 times lower than in Fig. 5, demonstrating almost linear propagation.

3. DISCUSSION AND CONCLUSIONS

The nonlinear numerical procedure applied here for the acoustic microscope made it possible to determine exactly the field distributions of strongly focused beams in the lens cavity and in the following region. Pressure value of $P_w^{'} = 1$ MPa, obtained by spectrum matching between the experimental and computed results (see Fig. 4) and by direct transducer measurements (giving $P_w^{''} = 0.79$MPa), seems to confirm with a good approximation the correctness of the applied procedure. This positive result was obtained in spite of some simplifying assumptions which were necessary to carry out the comparison.

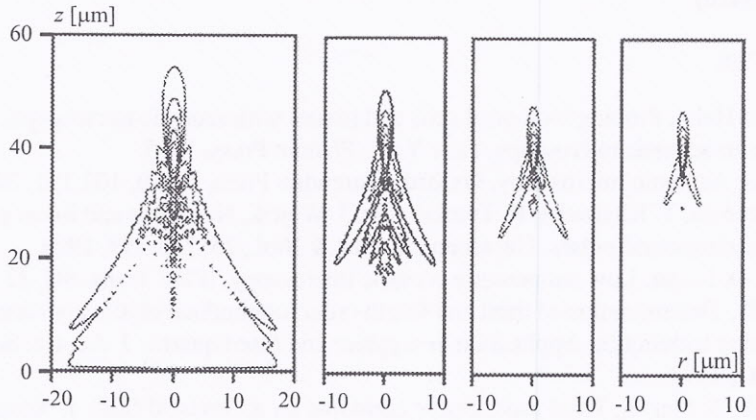

Fig. 8. Pressure distributions computed for the 1-st (from left to right), 2-nd, 3-rd and 4-th harmonics in the 1 GHz microscope field. Steps between contours are equal to 0.2 of the maximum value.

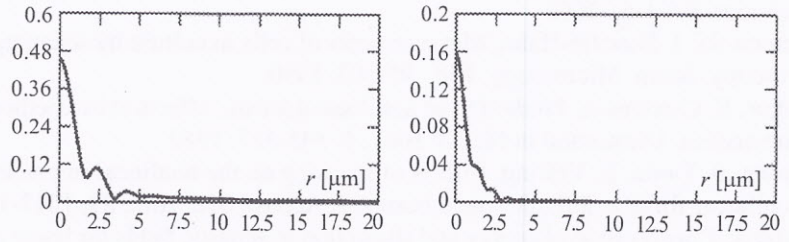

Fig. 9. Radial pressure distributions computed at the focus for the 1 GHz frequency (left) and for the second harmonic (right).

Fig. 5 shows the computed focal waveform distortions in water and the corresponding spectrum demonstrating a high number of harmonics. The maximum peak-to-peak pressure value obtained in the focus equalled 105 MPa for the maximum microscope power of 0.32 W [4], [2] (Table 1, line 12). Fig. 6 presents the axial distribution of the 1-st and 2-nd harmonics in this case. On the other hand, Fig. 7 shows the case of an almost linear propagation at a strongly reduced transducer power. All the other distributions were computed for the maximum transducer power. Fig. 8 shows pressure distributions in the lens focal region in the (z, r) presentation for the first 4 harmonics. The resolution obtained in the focus (Fig. 9) for the frequency of 1 GHz equalled 1.1 μm (-6dB) and 0.7 μm for the second harmonic.

Thus it was possible to determine many interesting data concerning pressure distributions,

effective focal cross-sections, intensity distributions, pulse waveform deformations and, as the next step, to establish the power density of heat sources, which enables to calculate the temperature increases important for examinations of living cells and tissues. In this way one can obtain a full description of nonlinear propagation effects in the acoustic fields of the microscopy that was previously lacking.

ACKNOWLEDGEMENTS

The authors thank the Committee of Scientific Research, Poland, for the financial support (Grant No 8T07B05420)

REFERENCES

1. J. Bereiter-Hahn, Probing biological cells and tissues with acoustic microscopy, Chapter 3, Advances in acoustic microscopy. New York: Plenum Press, 1995.
2. A. Briggs, Acoustic microscopy, Oxford, Clarendon Press, pp.30, 103,151, 303, 1992.
3. L. Filipczyński, T. Kujawska, R. Tymkiewicz, J. Wójcik, Nonlinear and linear propagation of diagnostic ultrasound pulses, Ultrasound in Med.& Biol., 25, 285-299, 1999.
4. J. Foster, D. Rugar, Low temperature acoustic microscopy, IEEE Trans. SU, 32, 139-51, 1985
5. Graham R., Determination of third and fourth order longitudinal elastic constants by shock compression techniques. Application to sapphire and fused quartz, J. Acoust. Soc. Am., 51, 1576-1581, 1972.
6. S. Kostek, B. Sinhua, Third order elastic constants for an inviscid fluid, J. Acoust. Soc. Am., 94,3014-3017, 1993.
7. J. H. Krautkrammer, Ultrasonic testing of materials, Springer, Berlin 1990.
8. P. Lewin, Test methodology and hydrophone calibration report, Sonic Consulting, Inc. Wyndmoor, PA 1-6, 2002.
9. J. Litniewski, J. Bereiter-Hahn, Measurements of cells in culture by scanning acoustic microscopy, Journ. Microscopy, 158, 95-107, 1990.
10. T. Muir, E. Carstensen, Prediction of nonlinear acoustic effects at biomedical frequencies and intensities, Ultrasound in Med.& Biol., 6, 345-357, 1980.
11. J. Tjotta, S. Tjotta, E. Vefring, Effects of focusing on the nonlinear interaction between two collinear finite amplitude sound beams, J. Acoust. Soc. Am., 89, 1017-1027, 1991.
12. J. Wójcik, Conservation of energy and absorption in acoustic fields for linear and nonlinear propagation, J. Acoust. Soc. Am., 104, 2654-2663, 1998.
13. J. Wójcik, A new theoretical basis for numerical simulations of nonlinear acoustic fields. In: Proceedings of the 15th International Symposium on Nonlinear Acoustics, Goettingen 1999, ed. American Society of Physics, 524, 141-144, 2000.
14. J. Wójcik, J. Litniewski, L. Filipczyński, Numerical and experimental determination of high nonlinearities in ultrasonic microscopy, Proc.17 Intern. Congress of Acoustics, Rome, paper 7B.02.02, 1-2, 2001.
15. J. Wójcik, J. Litniewski, L. Filipczyński, T. Kujawska, Nonlinear effects and possible temperature increases in ultrasonic microscopy, Archives of Acoustics, 27, 191-201, 2002.